Progress In Electromagnetics Research, Vol. 173, 141–149, 2022

Tamm States and Gap Topological Numbers in Photonic Crystals

Junhui Cao[1, 2], Alexey V. Kavokin[1, 2, *], and Anton V. Nalitov[3]

(*Invited Paper*)

Abstract—We introduce the concept of gap Zak or Chern topological invariants for photonic crystals of various dimensionalities. Specifically, we consider a case where Tamm states are formed at an interface of two semi-infinite Bragg mirrors and derive the formulism for gap Zak phases of two constituent Bragg mirrors. We demonstrate that gap topological numbers are instrumental in studies of interface states both in conventional and photonic crystals.

1. INTRODUCTION

Topological invariants, such as Zak numbers for one-dimensional spatial inversion symmetric crystals and Chern numbers for crystals with higher dimensions, are important characteristics of electronic states in crystal energy bands [1, 2]. Similarly, Zak and Chern numbers for photonic crystals characterise the properties of optical modes in allowed bands of such crystals [3–5]. Band topological numbers are typically introduced as integrals over the Brillouin zone in the reciprocal space [6, 7]. On the other hand, it is well known that eigen-states of electrons (photons) inside energy gaps of crystals (photonic crystals) can be characterised with Bloch-like functions and complex pseudo-wavevectors having physical meaning of attenuation length [8]. This enables one to introduce gap Zak and Chern numbers analogous to conventional Zak and Chern numbers, where the integration in the reciprocal space over the Brillouin zone is replaced with integration over the range of values taken by the complex pseudo-wavevectors of gap states as energy spans from the bottom to the top of the energy gap. To be specific, we consider an example of a structure formed by two semi-infinite one dimensional photonic crystals (Bragg reflectors). It is well known that localised optical modes referred to as optical Tamm states may be formed at the interfaces of different Bragg mirrors in some cases [9–11]. The concept of optical Tamm state was first established by Kavokin et al. [11] and observed by Sasin et al. [10]. It has been reported that optical Tamm states are important for the realization of vertical surface emitting lasers without the laser cavity [12, 13]. The eigen-energies of optical Tamm states belong to the photonic energy gaps of both mirrors. The magnitude of electromagnetic field in these modes decays exponentially in both directions from the interface. In practice, optical Tamm states have been used for the realization of one-dimensional planar topological lasers [14, 15]. Recently, the link between the emergence of optical Tamm states and Zak phases of allowed bands situated below and above the overlapping bandgaps of two one dimensional photonic crystals possessing the inversion symmetry has been discussed and studied [16, 17]. Here, we analysed a more general case of two photonic crystals, where inversion symmetry is not obeyed, derived the condition for Tamm states, and calculated the gap topological characteristic numbers.

Received 16 January 2022, Accepted 8 April 2022, Scheduled 22 April 2022

* Corresponding author: Alexey V. Kavokin (a.kavokin@westlake.edu.cn).

[1] Westlake University, 18 Shilongshan Road, Hangzhou 310024, Zhejiang Province, China. [2] Institute of Natural Sciences, Westlake Institute for Advanced Study, 18 Shilongshan Road, Hangzhou 310024, Zhejiang Province, China. [3] Faculty of Science and Engineering, University of Wolverhampton, Wulfruna Street, WV1 1LY, Wolverhampton, United Kingdom.

2. NUMERICAL DERIVATION OF TAMM STATES AND TOPOLOGICAL NUMBERS

2.1. Derivation of Tamm States

Let us consider the two photonic crystals with partially overlapping stopbands (a stopband is equivalent to the optical band gap [8]), addressed in [11]. The two types of layers are characterized with refractive indices $n_a = 1.4$ and $n_b = 2$, while their widths in the left and right crystals are given by a_l, b_l, a_r, and b_r, where $n_a a_l = 384\,\text{nm}$, $n_b b_l = 437\,\text{nm}$, $n_a a_r = 384\,\text{nm}$, $n_b b_r = 437\,\text{nm}$. Note that both structures deviate from the Bragg condition and are thus characterized by two types of stopbands opening at $k = 0$ and $k = \pi$.

We are focusing on the overlap of stop-bands of the left and right crystals. This configuration allows the freedom of choice of the two boundaries for each crystal, corresponding to the choice of their elementary cells. The latter may be set with two parameters z_l/d_l and z_r/d_r, where $z_l = n_a l_a$ and $z_r = n_a r_a$ are the optical lengths of layer a in the left and right crystals, respectively, with l_a and r_a being the width of layer a in left and right Bragg mirrors. $d_l = n_a a_l + n_b b_l$ and $d_r = n_a a_r + n_b b_r$ are the optical lengths of the left and right crystals, respectively. Both parameters z_l/d_l and z_r/d_r are spanning the range from 0 to 1 and fully define the boundary, as shown in Fig. 1(a). The first four photonic stopbands are shown in Fig. 1(b). The nodes in the stopbands are the consequence of Bragg condition, which is $z_l/d_l = \frac{i}{n-1}$, $i = 1, 2, 3\ldots$ for the n-th stopband. Note, however, that some structure configurations may correspond to different values of the parameters, in the case, where both crystal boundaries are of the same type.

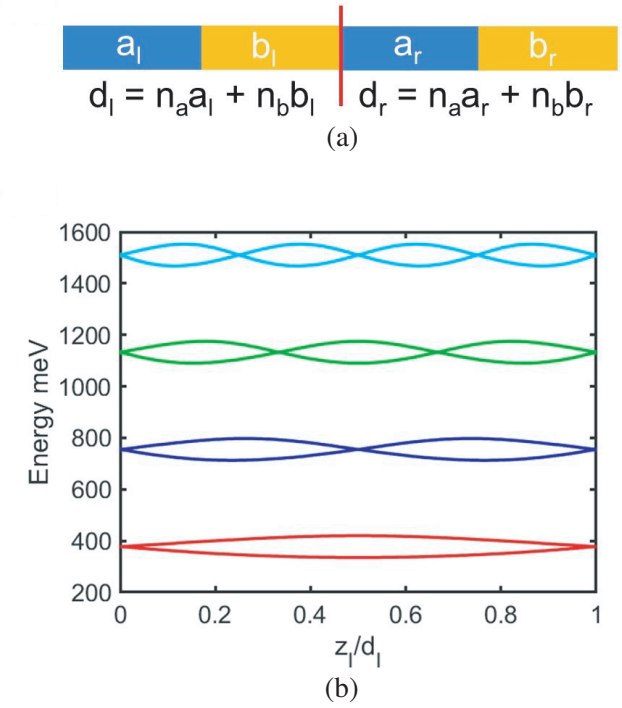

Figure 1. (a) The illustration of considered system. The widths of different optical layers in the Bragg mirrors are labeled by a_l, b_l, a_r, and b_r. The red line indicates the interface of the two semi-infinite Bragg mirrors. (b) Dependence of first four stopbands on z_l/d_l. Red, blue, green, cyan curves: boundaries of the first, second, third, and forth stopbands.

The condition on the existence of the interface state in terms of the reflection phases ϕ_l and ϕ_r, gained by the light reflected from the left and right semi-infinite crystals, reads simply $\varphi_l + \varphi_r = 0$.

These phases, in turn, may be found from the complex reflection coefficients

$$e^{i\varphi_{L(R)}} = r_{L(R)} = \frac{t_{12}^{L(R)} n - t_{11}^{L(R)} + X_{L(R)}}{t_{12}^{L(R)} n + t_{11}^{L(R)} - X_{L(R)}}, \tag{1}$$

where $t^{L(R)} < 1$ is the 2×2 transfer matrix of the left(right) structure period; $X_{L(R)}$ is its eigenvalue, corresponding to the state decaying from the boundary into the structure; and n is the refractive index of the environment, from where the light is incident. The equation $\varphi_L + \varphi_R = 0$ may be solved numerically, taking into account Eq. (1). Fig. 2 illustrates the result of the solution procedure spanning the space of parameters z_l/d_l and z_r/d_r, for different choices of Bragg mirrors in the left and right sides of the structure. Blue regions correspond to the parameters, for which the solution exists, in contrast to the yellow regions, where the solution is nonexistent in the energy overlap of the two stopbands. By tuning the total optical length of Bragg mirror, it is possible to compare two different stopbands in the same energy scale. For example, when matching the first stopband of left Bragg mirror with the second one in the right, we enlarge parameters $n_a a_r$ and $n_b b_r$ to twice the value. Hence, the energy of the second stopband in the right Bragg mirror is well matched with the first stopband in the left one. These diagrams of Tamm state exhibit the inversion symmetry with the inversion point $z_l/d_l = z_r/d_r = 0.5$. Besides, as Fig. 2 shows, Tamm states can be formed both between different stopbands (which is well-accepted) and between the same stopbands (for example, first-first and second-second stopbands).

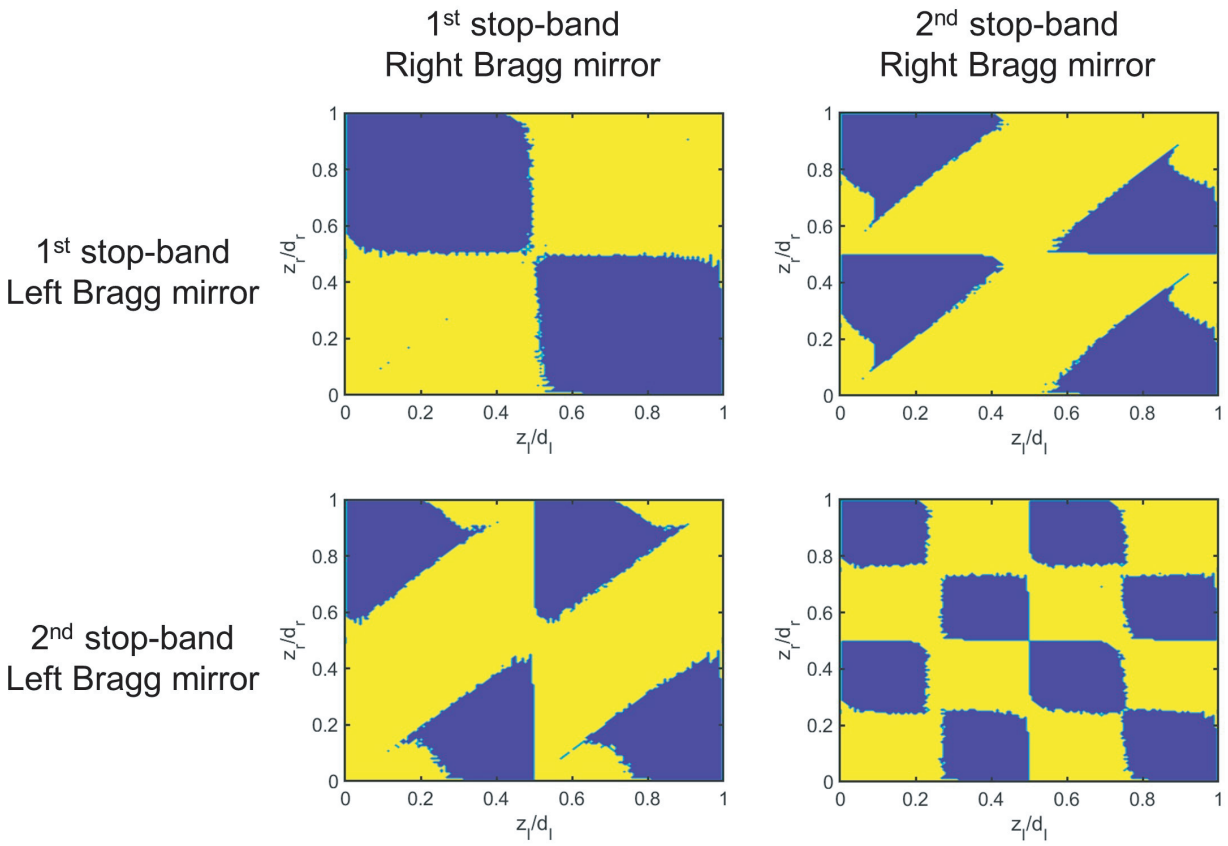

Figure 2. Diagrams showing the existence of Tamm states with different stop-bands. Blue regions indicate the structure in which a Tamm state can be formed, while yellow regions show structures where the Tamm state are forbidden.

2.2. Derivation of Topological Numbers

The presence of edge states in periodic structures may be related to the Zak phases, characterising energy bands situated below and above the stopbands that sustain the Tamm state [18]:

$$\gamma_n = i\int_{-\pi/d}^{\pi/d} A_n(k)dk, \tag{2}$$

where Berry connection A_n of the optical field in the absence of magnetoelectric coupling is defined as

$$A_n(k) = \int_0^d u_{n,k}(z)^* \frac{\partial}{\partial k} u_{n,k}(z)dz. \tag{3}$$

Here $u_{n,k}(z)$ is the periodic part of the n-th band Bloch function $E_{n,k}(z) = u_{n,k}(z)\exp(ikz)$. The latter may be computed with the transfer matrix approach as the first element of the vector

$$\begin{pmatrix} E_{n,k}(z) \\ cB_{n,k}(z) \end{pmatrix} = \mathrm{T}_k(z)\begin{pmatrix} E_{n,k}(0) \\ cB_{n,k}(0) \end{pmatrix}, \tag{4}$$

related to the n-th eigenvector across the period of the structure transfer matrix $T_k(d)$. The general transfer matrix of an optical layer can be written as

$$\mathrm{T} = \begin{bmatrix} \cos(\omega nL/c) & i\sin(\omega nL/c)/n \\ i\sin(\omega nL/c)n & \cos(\omega nL/c) \end{bmatrix}, \tag{5}$$

where ω is the frequency of electromagnetic wave transferring in the optical layer whose reflective indices and lengths are n and L, respectively.

The transfer matrix of layer a with width of d_a is

$$\mathrm{T_a} = \begin{bmatrix} \cos(\omega n_a d_a/c) & i\sin(\omega n_a d_a/c)/n_a \\ i\sin(\omega n_a d_a/c)n_a & \cos(\omega n_a d_a/c) \end{bmatrix}. \tag{6}$$

The transfer matrix of layer b with width of d_b is

$$\mathrm{T_b} = \begin{bmatrix} \cos(\omega n_b d_b/c) & i\sin(\omega n_b d_b/c)/n_b \\ i\sin(\omega n_b d_b/c)n_b & \cos(\omega n_b d_b/c) \end{bmatrix}. \tag{7}$$

The transfer matrix across the pair of layers $a-b$ with width of $d = d_a + d_b$, assuming that the layer a comes first,

$$\mathrm{T} = \mathrm{T_b}\cdot\mathrm{T_a} = \begin{bmatrix} t_{11} & t_{12} \\ t_{21} & t_{22} \end{bmatrix}, \tag{8}$$

where

$$\begin{aligned} t_{11} &= \cos(\omega n_a d_a/c)\cos(\omega n_b d_b/c) - \sin(\omega n_a d_a/c)\sin(\omega n_b d_b/c)\frac{n_a}{n_b} \\ t_{12} &= i\cos(\omega n_b d_b/c)\sin(\omega n_a d_a/c)/n_a + i\cos(\omega n_a d_a/c)\sin(\omega n_b d_b/c)/n_b \\ t_{21} &= i\cos(\omega n_a d_a/c)\sin(\omega n_b d_b/c)n_b + i\cos(\omega n_b d_b/c)\sin(\omega n_a d_a/c)n_a \\ t_{22} &= \cos(\omega n_a d_a/c)\cos(\omega n_b d_b/c) - \sin(\omega n_a d_a/c)\sin(\omega n_b d_b/c)\frac{n_b}{n_a} \end{aligned} \tag{9}$$

Applying the Bloch's theorem, two eigenvalues X of the 2×2 matrix T can be found as $X^{\pm} = e^{\pm ikd}$, where k is the pseudo-wavevector. The eigenvalues can also be expressed in terms of the period transfer matrix elements:

$$X^{\pm} = \frac{t_{11} + t_{22} \pm \sqrt{(t_{11}+t_{22})^2 - 4}}{2}. \tag{10}$$

Note that within the photonic band gap $|t_{11}+t_{22}| > 2$, rendering the eigenvalues real. At the same time, the expression for the complex reflection coefficient Eq. (1) depends on the eigenvalue, corresponding to the exponentially evanescent state, $X < 1$:

$$X = \frac{t_{11}+t_{22}}{2} - \mathrm{sgn}\left(\frac{t_{11}+t_{22}}{2}\right)\sqrt{\left(\frac{t_{11}+t_{22}}{2}\right)^2 - 1} \tag{11}$$

Eigenvectors corresponding to the two eigenvalues are

$$\begin{pmatrix} E_\omega(0) \\ cB_\omega(0) \end{pmatrix} = \begin{pmatrix} t_{12} \\ X - t_{11} \end{pmatrix}. \tag{12}$$

The electromagnetic field distribution inside the conventional unit cell is described by the transfer matrix

$$\begin{pmatrix} E_\omega(z) \\ cB_\omega(z) \end{pmatrix} = \mathrm{T}(z) \begin{pmatrix} E_\omega(0) \\ cB_\omega(0) \end{pmatrix}. \tag{13}$$

$\mathrm{T}(z)$ here is a piecewise matrix with $0 \le z \le d$. If $z \le d_a$,

$$\mathrm{T}(z) = \begin{bmatrix} \cos(\omega n_a z/c) & i\sin(\omega n_a z/c)/n_a \\ i\sin(\omega n_a z/c) n_a & \cos(\omega n_a z/c) \end{bmatrix}, \tag{14}$$

else if $d_a < z \le d$, we write $\mathrm{T}(z)$ as

$$\mathrm{T}(z) = \begin{bmatrix} t(z)_{11} & t(z)_{12} \\ t(z)_{21} & t(z)_{22} \end{bmatrix}, \tag{15}$$

with

$$\begin{aligned} t(z)_{11} &= \cos(\omega n_b(d-z)/c)\cos(\omega n_a d_a/c) - \sin(\omega n_b(d-z)/c)\sin(\omega n_a d_a/c)\frac{n_a}{n_b} \\ t(z)_{12} &= i\cos(\omega n_b(d-z)/c)\sin(\omega n_a d_a/c)/n_a + i\cos(\omega n_a d_a/c)\sin(\omega n_b(d-z)/c)/n_b \\ t(z)_{21} &= i\cos(\omega n_a d_a/c)\sin(\omega n_b(d-z)/c) n_b + i\cos(\omega n_b(d-z)/c)\sin(\omega n_a d_a/c) n_a \\ t(z)_{22} &= \cos(\omega n_b(d-z)/c)\cos(\omega n_a d_a/c) - \sin(\omega n_b(d-z)/c)\sin(\omega n_a d_a/c)\frac{n_b}{n_a}. \end{aligned} \tag{16}$$

Therefore, the expression of electric field in the optical unit cell is

$$E_\omega(z) = \begin{cases} t_{12}\cos(\omega n_a z/c) + i(X - t_{11})\sin(\omega n_a z/c)/n_a, & \text{if} \quad z \le d_a, \\ t_{12}\left[\cos(\omega n_b(d-z)/c)\cos(\omega n_a d_a/c) - \sin(\omega n_b(d-z)/c)\sin(\omega n_a d_a/c)\dfrac{n_a}{n_b}\right] & \\ +i(X - t_{11})\left[\cos(\omega n_b(d-z)/c)\sin(\omega n_a d_a/c)/n_a\right. & \\ \left.+\cos(\omega n_a d_a/c)\sin(\omega n_b(d-z)/c)/n_b\right], & \text{if} \quad d_a < z \le d \end{cases}. \tag{17}$$

In this way, the transfer matrix characterizing an entire optical unit cell is a serial multiplication of the unit cells' corresponding transfer matrices. We thus obtain the expression for the Berry connection in terms of the electric field defined by Eq. (4):

$$A_n(k) = \int_0^d E_{n,k}(z)^* \frac{\partial}{\partial k} E_{n,k}(z) dz - i\int_0^d |E_{n,k}(z)|^2 z dz. \tag{18}$$

Note that in Eq. (17) the expression for the electric field is implicit in the pseudo-wavevector k; however, it is explicit to the angular frequency ω of the electromagnetic wave. This is because the electric field was derived using transfer matrix, where the argument is ω, while what we want is the explicit expression of E_k towards k instead of ω, to calculate Berry connection. Therefore, we use one-to-one mapping between k and ω for each single allowed band, that is $kd = \arccos[(t_{11} + t_{22})/2]$. Thus the goal becomes to replace k in the formula of Berry connection by ω. To do this, we replace the argument k of Berry connection in Eq. (18) with ω, using the equation $k = \arccos[(t_{11} + t_{22})/2]/d = f(\omega)$,

$$A(f(\omega)) = \int_0^d E^*_{f(\omega)}(z) \frac{\partial}{\partial \omega} E_{f(\omega)}(z) \frac{\partial \omega}{\partial f(\omega)} dz - i\int_0^d |E_{f(\omega)}(z)|^2 z dz. \tag{19}$$

Here, $E_{f(\omega)}$ is found by replacing ω by $f(\omega)$ in the expression of E_ω. Finally, Zak phase γ is the integral of $A(k)$

$$\gamma = \int_{-\pi}^{\pi} dk A(k) = \int_{-\pi}^{\pi} df(\omega) A(f(\omega)) = \int d\omega \frac{df(\omega)}{d\omega} A(f(\omega)). \tag{20}$$

As $A(f(\omega))$ and $df(\omega)/\omega$ can be analytically expressed in the argument of ω, by integrating over the angular frequency from the allowed band's upper boundary to its lower boundary and then back to the upper one accounting for the change of sign in the expression for the eigen-value of the transfer matrix in Eq. (11) (identical to pseudo-wavevector from $-\pi$ to zero and then to π), the formula of Zak phase γ will be obtained.

Utilizing the Stock's theorem to calculate the topological invariant by Berry curvature in a 2D topological system works very well and eliminates the emergence of the gauge problem naturally [19, 20]. However, in a 1D optical lattice, the only available tool is Berry connection, which is a gauge dependent variable. Therefore, we applied the Wilson-loop approach to calculate the Zak phase [21–23]. By definition of the Berry connection (Eq. (3)), approximately we have

$$A_n(k_i) \approx \int_0^d dz \frac{u^*_{n,k_i}(z)\left[u_{n,k_{i+1}}(z) - u_{n,k_i}(z)\right]}{k_{i+1} - k_i} = \frac{\left\langle u_{n,k_i} | u_{n,k_{i+1}} \right\rangle - 1}{k_{i+1} - k_i} \tag{21}$$

with $k_{N+1} = k_1$ and $\langle u_{n,k_i} | u_{n,k_i} \rangle$ is normalized to 1 for any integer i from 1 to N. The inner product term gives Berry phase θ_i of the i-th segment:

$$e^{i\theta_i} = \left\langle u_{n,k_i} | u_{n,k_{i+1}} \right\rangle. \tag{22}$$

The entire Zak phase is an accumulation of the Berry phases from each small segment

$$e^{i\theta} = \prod_{i=1}^{N} \left\langle u_{n,k_i} | u_{n,k_{i+1}} \right\rangle. \tag{23}$$

As each Bloch function in above formalism has its complex conjugate multiplied, Eq. (23) is gauge-invariant. Finally, we can obtain the total Berry phase θ of optical unit cell by taking the logarithm of $e^{i\theta}$.

3. GAP ZAK PHASE

A conventional Zak phase is a characteristic topological property of allowed bands, obtained by integrating the Berry connection of the first Brillouin zone. To generalize this characteristic to photonic stopband, we introduce the *gap Zak phase* which is defined as an integral of the Berry connection of a stopband, with the path "bottom-top-bottom". Note that the eigen-frequency of light in a certain photonic stopband has a constant real part and an imaginary part varying with energy. In analogy with the integral over the first Brillouin zone where pseudo-wavevector is always real, the integral over stopband becomes the integral over the imaginary pseudo-wavevector. It allows us to use Eq. (3) without the loss of accuracy to calculate the Berry connection of a certain eigen-frequency, with the use of a complex pseudo-wavevector. It allows us to use Eq. (2) to calculate the Zak phase, by substituting the integral boundary as the imaginary pseudo-wavevector spans over the stopband:

$$\gamma_{sb} = i \oint_k A_{sb}(k) dk. \tag{24}$$

In this way, we can also define the Berry phase in stopbands with higher dimensions. For example, in a two-dimensional stopband, utilize Stokes' theorem,

$$\Omega_{sb}(k) = \nabla_k \times A(k) = \partial_x A_y(k) - \partial_y A_x(k), \tag{25}$$

where $\Omega_{sb}(k)$ is the Berry curvature. In a stopband, k is imaginary. Therefore, Berry phase in stopbands can be written as:

$$\gamma_{sb} = i \oiint_k \Omega_{sb}(\mathbf{k}) d\mathbf{k} = i \oiint_{k_x,k_y} \Omega_{sb}(k_x, k_y) dk_x dk_y, \tag{26}$$

where k_x and k_y are complex numbers in the stopband. In the case of a three-dimensional system, Eq. (24) may be used for calculating the Berry phase from Berry connection, where the integral path shall be a closed circuit in the 3D Brillouin zone. The gauge-invariant Berry curvature can be written as:

$$\mathbf{\Omega}_{sb}(k) = \nabla_k \times \mathbf{A}(k) = \Sigma_{\{abc\}} \epsilon_{abc} \partial_b A_c(k), \tag{27}$$

where ϵ_{abc} represents the Levi-Civita tensor. Finally, using the Stokes' theorem, we arrive at the expression of Berry phase γ_{sb} for the three-dimensional system:

$$\gamma_{sb} = i \int_{\boldsymbol{s}} \Omega_{sb}(\mathbf{k}) d\mathbf{S} \tag{28}$$

where $\boldsymbol{S}$ is the surface enclosed by the path in the integral of Berry connection. One can refer to γ_{sb} modulo 2π as to the gap Chern number. Note that, for a conventional optical crystal, the Zak phases of photonic allowed bands are usually numbers between zero and π, which brings difficulty in recognizing the topological property of the corresponding structure. Unlike the Zak phase of photonic allowed bands, which is 0 or π only for unit cells with inversion symmetry, the gap Zak number is also a Z_2 invariant for conventional unit cell. This characteristic of gap Zak number allows one to define the band gap as topologically trivial or nontrivial stopband.

Figure 3 shows the gap Zak phases of the first three stopbands. For the first stopband, the gap Zak phase is π for all configurations of z_l/d_l. For the even stopbands, it is trivial everywhere. The most interesting result of the gap Zak phase is in the third stopband, whose gap Zak phase is either π or zero. Moreover, the first jump from 0 to π occurs at the point of $z_l/d_l = 1/4$, which is the node for the forth stopband. Then a step down from π to 0 takes place at $z_l/d_l = 2/3 - 1/4$. This indicates that the node of the third stopband is the middle point of π-gap Zak phase. Similarly, the second plateau is centered around $z_l/d_l = 2/3$ and starts from $z_l/d_l = 1/3 + 1/4$ ending at $z_l/d_l = 3/4$. The concept of a gap Zak phase offers an opportunity to characterize the topology of localized electronic or photonic states in band gaps. Furthermore, the Z_2 symmetry protection of gap Zak phase is still valid in a conventional unit cell, while, in contrast, Z_2 symmetry is absent for Zak phases of allowed bands. This provides one with a tool to study the band topology in conventional photonic crystals.

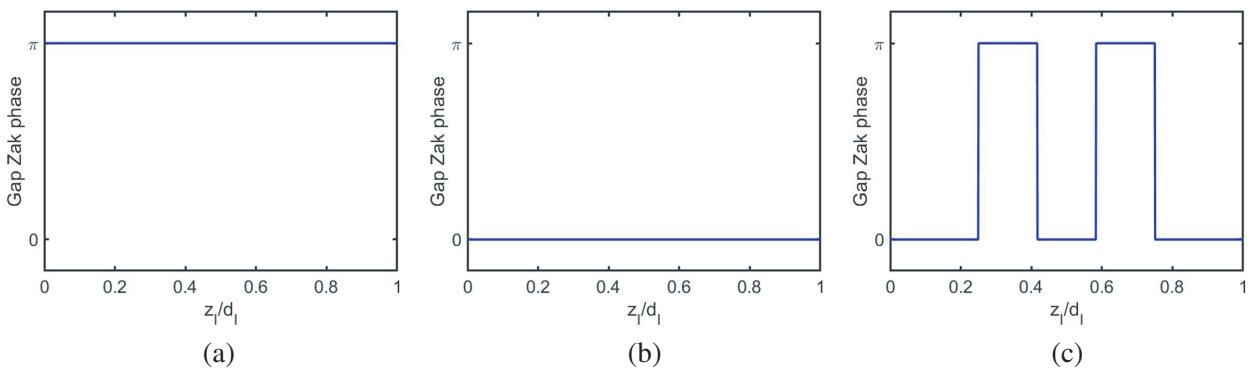

Figure 3. Gap Zak phases of (a) the first stop-band, gap Zak phase is π; (b) the second stop-band, the gap Zak phase is zero; (c) the third stop-band, the gap Zak phase is non-trivial around the Bragg condition points.

4. CONCLUSION

In summary, we established the concept of the gap topological number and showed the condition for the formation of a Tamm state. The gap Zak phase is nontrivial only for the odd stopbands in structures near the Bragg condition point, and zero for all even stop-bands. We also proved the existence of Tamm states in the overlapping stopbands characterized by the same real wavevector for two Bragg mirrors. We believe that our work will broaden the knowledge on topological photonic crystals and help the development of a topological polariton laser.

ACKNOWLEDGMENT

A. K. and J. C. are supported by the Westlake University, Project 041020100118 and Program 2018R01002 funded by Leading Innovative and Entrepreneur Team Introduction Program of Zhejiang Province of China.

REFERENCES

1. Xiao, D., M.-C. Chang, and Q. Niu, "Berry phase effects on electronic properties," *Rev. Mod. Phys.*, Vol. 82, 1959–2007, Jul. 2010.
2. Berry, M. V., "Quantal phase factors accompanying adiabatic changes," *Proc. R. Soc. Lond.*, Vol. 392, No. 1802, 45–57, 1996.
3. Qiang, W., X. Meng, L. Hui, S. Zhu, and C. T. Chan, "Measurement of the zak phase of photonic bands through the interface states of metasurface/photonic crystal," *Physical Review B*, Vol. 93, No. 4, 041415.1–041415.5, 2016.
4. Gao, W. S., M. Xiao, C. T. Chan, and W. Y. Tam, "Determination of zak phase by reflection phase in 1d photonic crystals," *Optics Letters*, Vol. 40, No. 22, 5259, 2015.
5. Ozawa, T., H. M. Price, A. Amo, N. Goldman, M. Hafezi, L. Lu, M. C. Rechtsman, D. Schuster, J. Simon, O. Zilberberg, and I. Carusotto, "Topological photonics," *Rev. Mod. Phys.*, Vol. 91, 015006, Mar. 2019.
6. Wang, F. and Y. Ran, "Nearly flat band with chern number $c = 2$ on the dice lattice," *Phys. Rev. B*, Vol. 84, 241103, Dec. 2011.
7. Hatsugai, Y., T. Fukui, and H. Aoki, "Topological analysis of the quantum hall effect in graphene: Dirac-fermi transition across van hove singularities and edge versus bulk quantum numbers," *Phys. Rev. B*, Vol. 74, 205414, Nov. 2006.
8. Kavokin, A., editor, *Microcavities. Number No. 16 in Series on Semiconductor Science and Technology*, Oxford University Press, Oxford, New York, 2007, OCLC: ocn153553936.
9. Afinogenov, B. I., V. O. Bessonov, A. A. Nikulin, and A. A. Fedyanin, "Observation of hybrid state of tamm and surface plasmon-polaritons in one-dimensional photonic crystals," *Applied Physics Letters*, Vol. 103, No. 6, 1800, 2013.
10. Sasin, M. E., R. P. Seisyan, M. A. Kalitteevski, S. Brand, R. A. Abram, J. M. Chamberlain, A. Y. Egorov, A. P. Vasil'Ev, V. S. Mikhrin, and A. V. Kavokin, "Tamm plasmon polaritons: Slow and spatially compact light," *Applied Physics Letters*, Vol. 92, No. 25, 824, 2008.
11. Kavokin, A. V., I. A. Shelykh, and G. Malpuech, "Lossless interface modes at the boundary between two periodic dielectric structures," *Physical Review B*, Vol. 72, No. 23, 233102, Dec. 2005.
12. Su, Y., C. Y. Lin, R. C. Hong, W. X. Yang, and R. K. Lee, "Lasing on surface states in vertical-cavity surface-emission lasers," *Optics Letters*, Vol. 39, No. 19, 2014.
13. Symonds, C., G. Lheureux, J. P. Hugonin, J. J. Greffet, and J. Bellessa, "Confined tamm plasmon lasers," *Nano Letters*, Vol. 13, No. 7, 3179, 2013.
14. Symonds, C., A. Lematre, E. Homeyer, J. C. Plenet, and J. Bellessa, "Emission of Tamm plasmon/exciton polaritons," *Applied Physics Letters*, Vol. 95, No. 15, 151114–151114-3, 2009.
15. Kavokin, A., I. Shelykh, and G. Malpuech, "Optical Tamm states for the fabrication of polariton lasers," *Applied Physics Letters*, Vol. 87, No. 26, 193, 2005.
16. Henriques, J. C. G., T. G. Rappoport, Y. V. Bludov, M. I. Vasilevskiy, and N. M. R. Peres, "Topological photonic Tamm states and the Su-Schrieffer-Heeger model," *Phys. Rev. A*, Vol. 101, 043811, Apr. 2020.
17. Xiao, M., Z. Q. Zhang, and C. T. Chan, "Surface impedance and bulk band geometric phases in one-dimensional systems," *Phys. Rev. X*, Vol. 4, 021017, Apr. 2014.
18. Zak, J., "Berry's phase for energy bands in solids," *Physical Review Letters*, Vol. 62, No. 23, 2747–2750, Jun. 1989.

19. Ryder, L. H., "The optical berry phase and the gauss-bonnet theorem," *European Journal of Physics*, Vol. 12, No. 1, 15, 1991.
20. Holstein, B. R., "The adiabatic theorem and Berry's phase," *American Journal of Physics*, 57, 1989.
21. Wang, H.-X., G.-Y. Guo, and J.-H. Jiang, "Band topology in classical waves: Wilsonloop approach to topological numbers and fragile topology," *New Journal of Physics*, Vol. 21, No. 9, 093029, Sep. 2019.
22. Gubarev, F. V. and V. I. Zakharov, "The Berry phase and monopoles in non-Abelian gauge theories," *International Journal of Modern Physics A*, Vol. 17, No. 02, 157–174, 2002.
23. Kondo, K.-I., "Wilson loop and magnetic monopole through a non-Abelian stokes theorem," *Physical Review D*, Vol. 77, No. 8, 284–299, 2008.